Canadian Mineralogist
Vol. 24, pp. 655-663 (1986)

PARABARIOMICROLITE, A NEW SPECIES, AND ITS STRUCTURAL RELATIONSHIP TO THE PYROCHLORE GROUP

T. SCOTT ERCIT*, FRANK C. HAWTHORNE AND PETR ČERNÝ
Department of Geological Sciences, University of Manitoba, Winnipeg, Manitoba R3T 2N2

ABSTRACT

Parabariomicrolite $BaTa_4O_{10}(OH)_2 \cdot 2H_2O$ is rhombohedral, space group $R\bar{3}m$, with a 7.4290(6), c 18.505(2) Å, V 884.5(1) Å, $Z = 3$. The strongest six lines in the X-ray powder pattern [d in Å(I)(hkl)] are 6.18(50)(00.3), 3.172(65)(02.1), 3.085(41)(00.6), 3.040(10.0)(20.2), 2.641(50)(02.4), 1.591(42)(22.6). Electron-microprobe analysis gives Na_2O 0.4, K_2O 0.3, SrO 0.8, BaO 10.5, PbO 0.4, Nb_2O_5 1.5, Ta_2O_5 80.6, $\Sigma = 94.5$ wt.%; crystal-structure arguments indicate 5.2 wt.% H_2O, to give a total $\Sigma = 99.7$ wt.%. Parabariomicrolite is translucent, white to pale pink, has a white streak and a vitreous to pearly lustre. It has well-developed {001} and {101} cleavages, is very brittle and has a Mohs hardness of 4; D(calc) 5.97 g/cm^3. It is optically anisotropic, with all n in excess of 2.0. Parabariomicrolite typically occurs as topotaxic replacements of microlite and more rarely as open-space fillings in oxide-mineral assemblages of the Alto do Giz pegmatite, Brazil. Its crystal structure was solved by crystal-chemical arguments, augmented by X-ray powder-diffraction data. Its layer structure is derived from that of pyrochlore. One layer has 6- and 3-membered rings of corner-sharing (TaO_6) octahedra, with [8]-co-ordinated Ba lying at the centre of the 6-membered rings; this layer is topologically identical with the analogous layer in pyrochlore. The second layer is very sparsely occupied by (TaO_6) octahedra; the analogous layer in pyrochlore is much more densely occupied (by large cations). It is the relative ordering of large cations in the first layer and vacancies in the second layer that result in the lowering of symmetry from $Fd3m$ to $R\bar{3}m$.

Keywords: parabariomicrolite, new mineral species, pyrochlore, crystal structure, tantalum oxide, Brazil, granitic pegmatite.

SOMMAIRE

La parabaryomicrolite $BaTa_4O_{10}(OH)_2 \cdot 2H_2O$ est rhomboédrique, groupe spatial $R\bar{3}m$, a 7.4290(6), c 18.505(2) Å, V 884.5(1) Å^3, $Z = 3$. Les six raies les plus intenses du cliché de poudre [d en Å(I)(hkl)] sont: 6.18(50)(00.3), 3.172(65)(02.1), 3.085(41)(00.6), 3.040(10.0)(20.2), 2.461(50)(02.4), 1.591(42)(22.6). L'analyse à la microsonde électronique a donné Na_2O 0.4, K_2O 0.3, SrO 0.8, BaO 10.5, PbO 0.4, Nb_2O_5 1.5, Ta_2O_5 80.6, total 94.5% en poids: des arguments cristallochimiques indiquent la présence de 5.2% d'eau, pour une somme de 99.7%. La parabaryomicrolite est translucide, blanche à rose pâle; elle a une rayure blanche et un éclat vitreux à perlé, des clivages {001} et {101} bien développées, et une dureté Mohs de 4. Elle est très cassante; D(calc) = 5.97. Optiquement anisotrope, tous ses indices de réfraction sont supérieurs à 2.0. On trouve la parabaryomicrolite en remplacement topotaxique de la microlite et, plus rarement, en remplissage de cavités dans les agrégats d'oxydes de la pegmatite de Alto do Giz, Brésil. Sa structure cristalline a été établie à partir de raisonnements cristallochimiques et des données de diffraction X sur poudre. C'est une structure en feuillets dérivée de celle du pyrochlore. Un premier feuillet comporte des anneaux de 6 et de 3 octaèdres (TaO_6), avec le baryum en coordinance 8 au milieu de l'anneau à six membres; ce feuillet est topologiquement identique à son analogue dans la structure du pyrochlore. Un deuxième feuillet, à population éparse, contient des octaèdres (TaO_6); le feuillet analogue du pyrochlore est occupé de façon beaucoup plus dense par des cations à large rayon. La ségrégation des gros cations dans le premier feuillet et des lacunes dans le second expliquent pourquoi la symétrie diminue de $Fd3m$ (pyrochlore) à $R3m$ (parabaryomicrolite).

(Traduit par la Rédaction)

Mots-clés: parabaryomicrolite, nouvelle espèce minérale, pyrochlore, structure cristalline, oxyde de tantale, Brésil, pegmatite granitique.

INTRODUCTION

During a general investigation of simpsonite parageneses, detailed examination of the Alto do Giz, Brazil, occurrence revealed a translucent white mineral; associated with the abundant microlite at this locality. Pough (1945) was the first to take note of the mineral; he referred to it as "altered microlite", but did not carry out X-ray, chemical or optical investigations. The mineral, characterized for the first time here, has been found to be a new species, very closely related to bariomicrolite (van der Veen 1963, Hogarth 1977) in chemistry. The mineral has been named *parabariomicrolite* in allusion to this relationship; the species and name have been approved for publication by the IMA Commission on New Minerals and New Mineral Names. Type material is housed in the collections of the Royal Ontario Museum, Toronto (M22607), and the Smithsonian Institution, Washington (NMNH 104739).

A mineral chemically similar to parabariomicrolite was found in a sample from near Lake Kivu, Zaire. On the basis of arguments to be presented in

*Present address: Mineral Sciences Division, National Museum of Natural Sciences, Ottawa, Ontario K1A 0M8.

later sections, this mineral is almost certainly a parabariomicrolite; however, because of the small size of the crystals (<30 μm), no X-ray-diffraction data could be collected for the confirmation of its identity.

Occurrence

The Alto do Giz pegmatite is located in the Brazilian Precambrian Shield, and is one of many Be,Ta,Li-bearing pegmatites in a 3750-km^2 belt centred about the Paraiba – Rio Grande do Norte border in the vicinity of Equador (De Almeida *et al.* 1944). Very little has been published on the geology of this region; available information is given by De Almeida *et al.* (1944) and Pough (1945).

The Alto do Giz is located 2 km S of the main road connecting the towns of Equador and Parelhas, in the state of Rio Grande do Norte, Brazil. The pegmatite dyke is hosted by a micaceous quartzite that overlies an inferred granitic batholith source, and has a vertical attitude (Pough 1945). Although heavily weathered, the pegmatite is well exposed at the crest of a ridge. It is zoned; published photographs and descriptions indicate the zoning to be horizontally symmetrical; the vertical zonation is not well documented. From descriptions of the horizontal zoning, there is a wall zone of quartz, mica and kaolinized feldspar. Progression toward the centre shows an intermediate zone(s) consisting mainly of coarser-grained quartz, feldspar and mica, followed by a quartz core. Beryl and Ta-oxide minerals occur in the intermediate zone, and tend to be concentrated in the innermost parts of this zone. A photograph presented by Pough (1945) indicates that large spodumene + quartz pseudomorphs after petalite are present in the intermediate zone; this brackets the formation of the intermediate zone at conditions of P between 2 and 4 kbar, T between 350 and 650°C (London 1984).

Tantalite is the dominant Ta-oxide mineral of the Alto do Giz pegmatite; however, large amounts of other Ta-oxide minerals were also found. Pough (1945), for example, reported that more than 300 kg of simpsonite $Al_4Ta_3O_{13}OH$ were mined in 1943, making Alto do Giz the world's largest deposit of this rare mineral. Quantities of the new species parabariomicrolite are by no means trivial; most microlite crystals from the Alto do Giz are slightly to completely altered to parabariomicrolite (Pough 1945), and some of the microlite crystals are up to 1 cm in diameter.

Because of the intense weathering of the pegmatite, the Ta-oxide minerals of the Alto do Giz pegmatite were found as loose crystals in kaolin; consequently, no direct information is available regarding the relationship of the oxide minerals to their original silicate associates. However, textural relationships between the Ta-oxide minerals are well preserved and indicate that manganotantalite, micro-

FIG. 1. Relict microlite (rounded islands) in a parabariomicrolite matrix. The greater polishing hardness of the microlite gives it a positive relief relative to parabariomicrolite.

lite, simpsonite and tapiolite represent an early generation. Later events, of probable hydrothermal character, resulted in the replacement of the simpsonite and microlite by natrotantite, alumotantite, stibiotantalite and parabariomicrolite.

X-Ray Crystallography

X-ray powder-diffraction patterns were obtained by Debye-Scherrer and Gandolfi methods, on powders and crystal fragments, respectively, and by powder diffractometry. Extreme variability of the first Debye-Scherrer and Gandolfi patterns indicated contamination by a second phase. However, the variability made identification and characterization of each phase easier. The contaminant phase is microlite, which, by later inspection of polished sections, was found as minute relics in areas initially suspected to be pure parabariomicrolite (Fig. 1).

Precise *d*-values were determined by X-ray powder diffractometry using a Philips PW1030 diffractometer and Ni-filtered Cu$K\alpha$ radiation. After calibration against quartz, diffraction maxima corresponding to the microlite contaminant were eliminated from the data set. The remaining pattern resembles those of the pyrochlore-group minerals, except that several diffraction-maxima in the pattern are "split", starting at very large values of *d* [*e.g.*, the "split" pair with *d* values of 6.17 and 6.08 Å corresponds to *d*(111) of microlite]. The splitting suggests a lower than cubic symmetry; by trial and error, the pattern was indexed on a rhombohedral cell. Although the presence of the microlite contaminant complicated the diffraction pattern, comparison with a pattern for pure Alto do Giz microlite made peak assignment unambiguous; consequently, unit-cell parameters for both phases of the pattern could be determined.

Initially the parabariomicrolite was indexed on a rhombohedrally distorted *F*-centred pyrochlore cell. This gave *a* 10.5657(5) Å, α 89.358(6)°. No diffraction maxima violate the *F*-centring of this setting. The pattern was then re-indexed on a conventional *R*-centred cell with hexagonal axes, giving *a* 7.4290(6), *c* 18.505(2) Å. Indexed powder-diffraction data for this setting are given in Table 1.

Precession photographs (0 to 2nd levels) of parabariomicrolite very strongly resemble those of microlite. No reflections were found that violate the F-centring of the pyrochlore-like setting. However, of the five sets of photographs collected on five apparently single crystals of parabariomicrolite, two show evidence of microlite contamination, and these plus two more show large, elongate diffraction-maxima characteristic of twinning or mosaic structure. The photographs with microlite contamination show a topotaxic relationship between parabariomicrolite and microlite, with {001}and {101} of parabariomicrolite parallel to {111} of microlite.

TABLE 1. X-RAY POWDER-DIFFRACTION DATA FOR PARABARIOMICROLITE

hkl	d (calc)	d (obs)	I	hkl	d (calc)	d (obs)	I
00.3	6.17	6.18	50	10.10	1.778	1.778	20
10.1	6.08	6.09	35	22.3	1.778		
01.2	5.28	5.28	6	12.8	1.676	1.675	3
10.4	3.76	3.76	3	01.11	1.628	1.628	3
11.0	3.71	3.71	2	02.10	1.604	1.603	24
01.5	3.208	3.207	7	40.1	1.602		
02.1	3.169	3.172	65	22.6	1.591	1.591	42
00.6	3.084	3.085	41	40.4	1.519	1.519	14
20.2	3.038	3.040	100	20.11	1.491	1.491	4
02.4	2.641	2.641	50	30.9	1.484	1.484	2
20.5	2.428	2.426	13	04.5	1.475	1.474	6
11.6	2.373	2.371	3	21.10	1.473		
12.2	2.352	2.353	1	22.9	1.378	1.379	8
21.4	2.152	2.152	5	04.8	1.321	1.320	7
00.9	2.056	2.056	7	20.14	1.223	1.223	4
02.7	2.042	2.043	10	40.10	1.214	1.214	9
30.3	2.026	2.025	10	33.3	1.214		
20.8	1.878	1.878	38	42.2	1.205	1.205	14
22.0	1.857	1.857	39	22.12	1.186	1.187	10
11.9	1.799	1.798	5	24.4	1.176	1.176	10
21.7	1.790	1.789	3				

a = 7.4290(6) c = 18.505(2) Å

Philips powder diffractometer, 1° divergence slit, Ni-filtered CuKα radiation. Internal standard: quartz. Integrated intensities.

Measurements on the four sets of precession photographs with smeared diffraction-maxima show a metrically cubic cell, but Gandolfi photographs of the same fragments gave patterns with line splitting characteristic of rhombohedral parabariomicrolite. The remaining set of precession photographs, with sharp diffraction-maxima, show evidence of rhombohedral symmetry in terms of reciprocal *d*, interreciprocal axis angles and diffraction intensities. For the 10.5-Å *F*-centred microlite-like cell, an α angle of 89.26±0.10° was measured, close to the value of 89.358(6)° refined from powder data. However, smearing of the diffraction maxima within circles of constant $\sin\theta/\lambda$ suggests that this sample is slightly twinned or shows slight mosaic character.

Twinning is the likely cause of most smeared diffraction-maxima. Topotaxic control over replacement of microlite by parabariomicrolite could produce four-fold parabariomicrolite twins: the *Z* axis of parabariomicrolite corresponds to the body diagonal {111} of microlite; there are four symmetrically equivalent body diagonals in microlite; four-fold twinning should result in parabariomicrolite that topotaxically replaces microlite. With only a (90–89.36=) 0.64° angular deviation from cubic metricity, twinning coupled with the poor crystallinity of the sample might easily produce oversized, elongate maxima, rather than the resolved multiple diffraction-maxima normally expected in a twinned pattern.

According to powder-diffraction and precession-photograph data, conditions of systematic absence for parabariomicrolite are hkl with $-h+k+l=3n+1$, giving $R\bar{3}m$, $R3m$, $R32$ and $R3$ as possible space-groups (all are subgroups of $Fd3m$). Even the diffraction pattern of the crystal of parabariomicrolite with the sharp diffraction-maxima has $\bar{3}m$ diffraction symmetry; thus $R\bar{3}m$, $R3m$ and $R32$ are the most probably choices for the space group of parabariomicrolite.

Physical and Optical Properties

Parabariomicrolite is translucent, white to pale pink and has a white streak. The lustre ranges from vitreous to pearly. The mineral is nonfluorescent under both short- and long-wave ultraviolet light. Parabariomicrolite is slightly softer than its associated microlite; it has a hardness of 4 and is very brittle. This, coupled with well-developed {001} and {101} cleavages, causes the mineral to splinter under even the slightest pressure. It is anisotropic and has all indices of refraction greater than 2.0 (Gladstone-Dale calculations give $\bar{n}=1.96$). Further optical investigations met with failure due to the high indices of refraction, the tendency of the mineral to splinter upon removal from polished sections, its translucency, and the small size of the regions of pure parabariomicrolite. Samples were either too small or too contaminated with microlite for a density determination; however, the density calculated from the proposed formula is 5.97 g/cm^3, in good agreement with a measured density of 6.03 g/cm^3 for a parabariomicrolite–microlite mixture (Pough 1945).

Parabariomicrolite typically occurs as topotaxic replacements of microlite; however, some samples seem to be open-space fillings. The size of individual crystals ranges from 0.01 to 0.1 mm; aggregates of crystals are up to 2 mm across.

Chemical Composition

Parabariomicrolite was chemically analyzed using a MAC 5 electron microprobe operating in the wavelength-dispersion (WD) mode at an accelerating voltage of 20 kV and a sample current of 40 nA measured on chromite. The following standards were used: microlite (Ta$L\alpha$, Nb$L\alpha$, Na$K\alpha$), $Ba_2NaNb_5O_{15}$ (Ba$L\alpha$), $SrTiO_3$ (Sr$K\alpha$), PbTe (Pb$L\alpha$) and orthoclase (K$K\alpha$). Ca, Ti, Sn and U were also sought but were not detected. A modified version of the EMPADR VII program (Rucklidge & Gasparrini 1969) was used for data reduction. The parabariomicrolite-like mineral from Lake Kivu was analyzed in the energy-dispersion (ED) mode using the same microprobe as above, but a Kevex Micro-X 7000 spectrometer and Kevex software utilizing the MAGIC V program (Colby 1980) were used in data collection and reduction. Operating conditions were 15 kV, 5 nA and involved a 200 live-second collection time for the sample spectrum; standard spectra were collected until counts from lines intended for analysis were precise to 1–5%, depending upon the line in question. The same standards were used as listed above, except that microlite was also used for Ca analysis ($K\alpha$ line). Minor overlaps of lines, *e.g.*, TaM upon NbL and *vice versa*, were dealt with by energy-stripping techniques. The absence of Ti was confirmed by a WD scan of the region about the TiK peaks; thus Ba–Ti overlap was not a problem in the ED analysis.

TABLE 2. CHEMICAL COMPOSITION* OF PARABARIOMICROLITE AND ASSOCIATED MICROLITE

		1	2	3
Na_2O	wt.%	0.4	0.0	5.3
K_2O		0.3	0.0	0.0
CaO		0.0	1.7	8.1
SrO		0.8	0.0	0.0
BaO		10.5	7.3	0.0
PbO		0.4	3.4	1.2
Nb_2O_5		1.5	9.0	1.7
Ta_2O_5		80.6	70.9	81.7
		94.5	92.3	98.0
	Unit-Cell Contents (on 12 B cations)			
Na		0.40	0.00	5.37
K		0.22	0.00	0.00
Ca		0.00	0.91	4.53
Sr		0.23	0.00	0.00
Ba		2.19	1.48	0.00
Pb		0.06	0.47	0.17
Nb		0.36	2.09	0.40
Ta		11.64	9.91	11.60
		15.10	14.86	22.06
O (eff)		32.82	32.86	37.39

*determined by electron-microprobe analysis.
1. Parabariomicrolite, Alto do Giz, Brazil (M22607).
2. Parabariomicrolite, Lake Kivu, Zaire (NMNH 136445).
3. Microlite, Alto do Giz (M22607).

The composition of parabariomicrolite and the parabariomicrolite-like mineral are given in Table 2, as well as that of an unreplaced microlite relic in the parabariomicrolite (WD).

Microlite typically contains 2–3 wt.% H_2O+F; thus in the absence of H_2O and F determinations, the analytical sum of 98.0 wt.% for the microlite inclusion is well within expectations. The total for the parabariomicrolite analysis is 3.5 wt.% lower than that of the microlite. Because both analytical data-sets were obtained at the same time, the same operating conditions apply to the analyses; thus the 3.5 wt.% difference should be a reasonable estimate

of the difference in volatile content of the two minerals. Furthermore, with the reasonable analysis of microlite available as a check, some confidence can be placed on the estimate of the H_2O+F content of parabariomicrolite as 5.5 wt.% by difference.

The work of Eid & von Knorring (1976) on microlite geochemistry has shown that the $F:(OH+H_2O)$ ratio of pegmatitic microlite is geochemically controlled. Primary pegmatite-hosted microlite, which is typically found as disseminations in lithian mica units, in albitic units or as pocket constituents, belongs to the group richest in F. Secondary microlite, which occurs as a replacement of other tantalum oxides, is typically F-impoverished, and commonly enriched in H_2O, as opposed to OH. Textural evidence shows that parabariomicrolite is a secondary microlite-like mineral; hence it is reasonable to assume that most (if not all) of the undetected constituents of parabariomicrolite consist of H_2O+OH. Water-rich (as opposed to hydroxyl-rich) microlite is typically poorly crystalline; the poor crystallinity of parabariomicrolite may indicate that much of the H_2O is actually structural water. Alternatively, the poor crystallinity may be due to metamictization; however, (1) no uranium has been detected in any of the minerals of the Alto do Giz occurrence of the simpsonite paragenesis, and (2) none of the microlite of the simpsonite paragenesis, including the microlite relics in the parabariomicrolite, shows poor crystallinity. Thus the poor crystallinity of the parabariomicrolite is most likely related to high content of water.

Parabariomicrolite is essentially a barium tantalum oxide mineral; however, minor amounts of Pb, Sr, Na and K substitute for Ba, and Nb substitutes for Ta. In terms of trace and minor elements, the mineral is similar to microlite encountered in the simpsonite paragenesis, especially in its Pb-enrichment and lack of Ti.

In the absence of a reliable measured density for parabariomicrolite, the unit-cell contents of the mineral were determined by assuming a pyrochlore-like structure for the mineral. More specifically, a BO_6 octahedral framework topologically identical to that of pyrochlore-group minerals is expected on the bases of 1) the topotaxic relationship of parabariomicrolite to the microlite it replaces, and 2) the strong similarity of the X-ray-diffraction patterns of parabariomicrolite and pyrochlore-group minerals. The unit-cell volume of parabariomicrolite is ¼ times that of the pyrochlore structure: thus parabariomicrolite has $16 \times \frac{1}{4} = 12$ *B* cations per unit cell. The unit-cell contents of Table 2 were calculated on this basis.

The sum of the mono- and divalent cations, which shall hereafter be called *A* cations, is equal to 3. From Table 2, the effective number of oxygen atoms for charge balance is 32.82; however, to meet the expectation of a pyrochlore-like octahedral framework, there must be at least $48 \times \frac{1}{4} = 36$ anions (with a possibility of $8 \times \frac{1}{4} = 6$ more at the ϕ site). Thus, by analogy with synthetic pyrochlores, an appreciable amount of OH must be present even at the former O-site in order to raise the number of anions to 36. This is in line with the high (H_2O+F) content of the parabariomicrolite suggested by the analytical sum of 94.5 wt.%.

Crystal Structure

The limited data available for parabariomicrolite leave the discussion of the crystal chemistry of the mineral at an unsatisfactory point. The exact relationship of the structure of the mineral to that of pyrochlore, and the conditions for the stable crystallization of parabariomicrolite *versus* bariomicrolite are unknown. Based on systematic absences in the powder-diffraction data, there are as many as five possible space-groups for parabariomicrolite. Group-subgroup relationships do not help to reduce this number; all possible space-groups are subgroups of $Fd3m$. With no suitable single crystals available for structure analysis, nor enough powder available for quantitative Rietveld refinement, neither single-crystal nor powder-diffraction methods of structure analysis were possible. Consequently, a trial-and-error approach was taken to structure solution.

The first step of the solution involved the transformation of co-ordinates of the pyrochlore structure (*F*-centred, cubic) to a hexagonal-*R* basis. The following transformation-matrix was derived:

$$\left[\begin{matrix} -\frac{4}{3} & -\frac{2}{3} & \frac{2}{3} \end{matrix} \middle/ \begin{matrix} -\frac{2}{3} & -\frac{2}{3} & \frac{4}{3} \end{matrix} \middle/ \begin{matrix} \frac{1}{3} & \frac{1}{3} & \frac{1}{3} \end{matrix}\right]$$

Because of the high symmetry of the pyrochlore structure, and of the relatively simple cation chemistry of parabariomicrolite, the highest-symmetry space group possible for parabariomicrolite ($R\bar{3}m$) was initially chosen, with the intention of using lower-symmetry space groups only if necessary. Site correlations for the pyrochlore structure in its $Fd3m$ setting and in the transformed setting ($R\bar{3}m$) are given in Table 3.

The $Fd3m \rightarrow R\bar{3}m$ transformation causes each site of the cubic structure of pyrochlore to split into two nonequivalent sites, except for the ϕ site. Both the *A* and *B* sites split into one site with a multiplicity of 9 and one with a multiplicity of 3. With a sum of 3 *A* cations per unit cell, it is an appealing possibility that all *A* cations are ordered in the threefold site (denoted *A*) and all (pyrochlore) *A*-site vacancies in the ninefold site (denoted A^*). Alternatively, it may be that the *A* cations remain disordered over

TABLE 3. SITE CORRELATION BETWEEN Fd3m AND R3m PYROCHLORE

	Fd3m Pyrochlore					R3m Pyrochlore				
Atom	Site	Posi-	x	y	z	Site	Posi-	x	y	z
Ba	A	16d	1/2	1/2	1/2	A	3b	0	0	1/2
						A*	9e	1/2	0	0
Ta	B	16c	0	0	0	B1	3a	0	0	0
						B2	9d	1/2	0	1/2
O	O	48f	x	1/8	1/8	O1	18h	x	-x	z
						O2	18h	x	-x	z
OH, F, H_2O	ϕ	8b	3/8	3/8	3/8	ϕ	6c	0	0	z

both sites, each having a fractional occupancy of 0.25. However, unlike the former model, the latter does not account for the rhombohedral symmetry of the mineral. Furthermore, for isotropically vibrating atoms, the latter model predicts zero intensity for reflections such as (01.2), (10.4), (11.0), (11.6) and (12.2); however the diffraction maxima have readily observable intensities [*e.g.*, $I(01.2) = 6\%$, Table 1]. It would seem that even at this stage, the ordered *A*-cation model is to be preferred.

An attempt was made to refine the positional parameters of the structure initially from bond-valence considerations, and subsequently by comparison with the reflection intensities of the powder data listed in Table 1. Because of the paucity of data, the BO_6 framework of the structure was constrained to obey cubic symmetry. This places constraints on the *x* and *z* parameters of O1 and O2; from the $Fd3m - R\bar{3}m$ transformation matrix,

$$x(O1) = x(O2) = \tfrac{2}{3}\, x(O^*) - 1/12 \qquad (1)$$

$$z(O1) = \tfrac{1}{3}\, x(O^*) + 1/12 \qquad (2)$$

$$z(O2) = \tfrac{1}{3}\, x(O^*) + 5/6 \qquad (3)$$

thus: $x(O1) = x(O2) = 2\,z(O1) - \tfrac{1}{4} = 2\,z(O2) - 7/4 \qquad (4)$

where the sites marked by asterisks are for the pyrochlore structure and those without asterisks are for the parabariomicrolite structure. The above assumption reduces the number of independent positional variables for O1 and O2 of the parabariomicrolite structure from 4 to 1. Because the *B*-cation polyhedra of parabariomicrolite are co-ordinated by only O1 and O2, *x*(O1) can be refined by minimizing the differences between the expected and observed bond-valences at *B*1 and *B*2. Refinement gave $x(O1) = 0.1253$ for $\Sigma s(B1) = 5.00$ v.u., $\Sigma s(B2) = 5.00$ v.u., thus $x(O2) = 0.1253$, $z(O1) = 0.1877$, and $z(O2) = 0.9377$, from equation (4).

TABLE 4. OBSERVED AND CALCULATED DIFFRACTION INTENSITIES FOR PARABARIOMICROLITE

hkl	I(obs)	I(calc)		
		1	2	3
00.3	50	73	81	26
10.1	35	53	57	76
01.2	6	8	11	0
10.4	3	7	7	0
11.0	2	5	3	0
01.5	7	6	8	16
11.3	65	66	55	38
00.6	41	40	35	35
20.2	100	100	100	100
02.4	50	49	47	42
20.5	13	16	13	3
11.6	3	4	3	0
12.2	1	2	3	0
21.4	5	5	6	0
00.9	7	6	6	3
02.7	10	8	8	2
30.3	10	8	3	11
20.8	38	28	28	30
22.0	39	31	27	14
11.9	5	4	3	5
21.7	3	4	3	2
10.10	20	18	18	9
12.8	3	2	2	0
01.11	3	1	1	3
31.5	24	24	23	21
22.6	42	45	42	42
40.4	14	12	12	11
20.11	4	6	5	2
30.9	2	3	2	3
13.7	6	6	5	2
22.9	8	6	6	3
04.8	7	8	8	8

1: All Ba ordered into A site. ϕ site fully occupied.
2: All Ba ordered into A site. ϕ site vacant.
3: Ba disordered over A & A* sites. ϕ site fully occupied.

TABLE 5. SELECTED DISTANCES (Å) AND ANGLES (°) FOR THE PARABARIOMICROLITE STRUCTURE

A Polyhedron	B1 Polyhedron	B2 Polyhedron
BOND LENGTHS		
A - O1 x6 2.71	B1 - O2 x6 1.98	B2 - O1 x4 1.97
- ϕ x2 3.33		- O2 x2 2.00
< A - O > 2.87		< B2 - O > 1.98
ANGLES		
O1 - A - O1 x6 118	O2 - B1 - O2 x6 90	O1 - B2 - O1 x2 90
- O1 x6 62	- O2 x6 90	- O1 x2 90
- ϕ x6 98	< O - B1 - O > 90	- O2 x4 89
- ϕ x6 82		- O2 x4 91
< O - A - O > 90		< O - B2 - O > 90
O-O DISTANCES		
O1 - O1 x6 2.79*	O2 - O2 x6 2.79	O1 - O1 x2 2.79*
- ϕ x6 3.98	- O2 x6 2.81	- O1 x2 2.79*
< O - O > 3.39	< O - O > 2.80	- O2 x4 2.80
		- O2 x4 2.83
		< O - O > 2.81

"*" denotes shared polyhedral edges

TABLE 6. BOND VALENCES* FOR PARABARIOMICROLITE

A Octahedron		B1 Octahedron		B2 Octahedron	
Bond	s	Bond	s	Bond	s
A-O1 x6	0.32	B1-O2 x6	0.84	B2-O2 x4	0.86
-ϕ x2	0.05			-O2 x2	0.78

Site Sums

A: 2.0	B1: 5.0	B2: 5.0
O1: 2.0	O2: 1.6	ϕ: 0.1

*bond valences in valence units (v.u.)

The only other positional parameter $z(\phi)$ is model-dependent; thus different criteria were used to determine its value for the different models. In the case of the ordered-Ba model, *i.e.*, with all Ba at *A*, $z(\phi)$ was determined by normalizing the bond-valence sum for *A* to a value of 2. This gave $z(\phi) = 0.315$. For the model with disordered Ba, the ϕ site was set at the ideal location for the pyrochlore structure, *i.e.*, at $z(\phi) = \frac{1}{8}$.

Diffraction intensities for each model were calculated using the program DBW 2.9 (Wiles & Young 1981), and are compared to the observed intensities in Table 4. Casual examination of Table 4 shows the ordered model (1) to be greatly superior to the disordered model (3). The reflections with calculated intensity of zero alluded to earlier are given in this table, and further emphasize the problems of the disordered model. On a more objective level, Bragg *R*-indices were calculated for each model by: $R = \Sigma|I_o - I_c|/\Sigma I_o$. The resulting indices are $R = 16\%$ for the ordered model and $R = 36\%$ for the disordered model. Because of the small sample-size coupled with the large divergence of the incident X-ray beam at low-2θ angles, the beam was much larger than the sample at low angles, thus the models significantly overestimate the intensities of large-*d* diffraction maxima. The effect of this unavoidable systematic error was reduced by repeating the calculation using only reflections with *d* values less than 4.0 Å. The resulting values were $R = 11\%$ and $R = 29\%$ for the ordered and disordered models, respectively. For both approaches to the calculation, the ordered model is clearly superior to the disordered one.

Bond lengths, angles and O–O separations for the ordered model are given in Table 5. Bond valences are given in Table 6. The bond-valence sum to O1 of 2.0 v.u. indicates that O1 is occupied only by O. The sum to O2 of 1.6 v.u. indicates that all of the OH in the BO_6 framework is located at this site. The sum to ϕ of 0.1 v.u. is instructive. A typical bond-valence for O–H bonds in solids is 0.8 v.u. (Brown 1981); thus, neglecting the contribution of O–H bonds, the sum to an oxygen of an H_2O molecule is $2 - (2 \times 0.8) = 0.4$ v.u., whereas it is $2 - 0.8 = 1.2$ v.u. for the O of a hydroxyl molecule. The very low sum to ϕ indicates that either ϕ is occupied by H_2O, or not occupied at all. Important in this regard is the observation that parabariomicrolite has a total volatile content of 5.5 wt.%. With the expectation of full occupancy of the O sites, the effective number of oxygen atoms per unit cell of 32.82 gives 18 O at the O1 site and 11.64 O + 6.36 OH at the O2. This OH corresponds to 1.8% H_2O by weight, significantly less than the amount expected from the analysis deficit in the sum. Only by introducing H_2O molecules at the ϕ site can this figure be increased. If the ϕ site is fully occupied by H_2O, then 5.2 wt.% H_2O results, which would give an excellent analytical sum of 99.7 wt.%.

As a further test of the ϕ-site occupancy, a second calculation of intensity was carried out, this time modeling ϕ as vacant (column 2 of Table 4). *R*

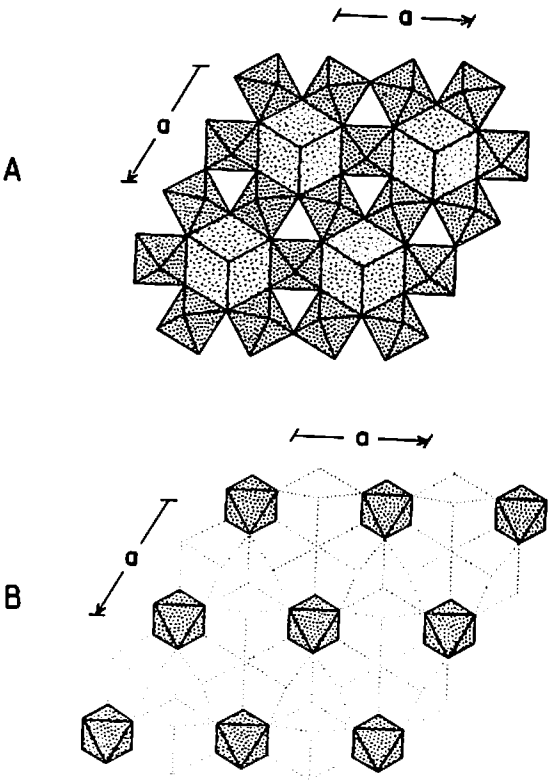

FIG. 2. The layer structure of parabariomicrolite. (A) Layer 1: *B*2-cation polyhedra are stippled; *A*-cation polyhedra are hatch-stippled. (B) Layer 2: *B*-cation polyhedra are stippled; unoccupied polyhedra are represented with a dotted outline.

indices were $R = 21\%$ for all diffraction maxima and $R = 14\%$ for those maxima with d less than 4.0 Å, giving 5% and 3% poorer fits, respectively, than the same calculations with ϕ fully occupied by H_2O.

It is concluded that for the site labels of Table 3, A is occupied by Ba (and Na, Pb, Sr, K), A^* is vacant, $B1$ and $B2$ are occupied by Ta (and Nb), O1 by O, O2 by O + OH and ϕ by H_2O. The ideal chemical formula for parabariomicrolite thus is: $BaTa_4O_{10}(OH)_2 \cdot 2H_2O$ ($Z = 3$).

If the O plus OH of the O2 site are ordered, instead of disordered, then the space-group symmetry must be lower than $R\bar{3}m$. With approximately 6 OH and 12 O at O2, a 1:2 splitting of the site would be expected. None of the R-centred subgroups of $R\bar{3}m$ allow splitting of O2 in this fashion; it is concluded that $R\bar{3}m$ is the best candidate for the space group of parabariomicrolite, and that the O and OH are disordered over O2.

Description of the Structure

The parabariomicrolite structure is shown in Figure 2. It is best described as a layer structure, consisting of alternations of two topologically distinct layers along Z, as has been done previously for the pyrochlore structure (along {111}: Yagi & Roth 1978). One layer (Fig. 2a) has corner-sharing BO_6 octahedra (B site) that form 6- and 3-membered rings within the layer. This layer has a topologically identical counterpart in the pyrochlore structure. A cations are located at the geometric centre of the 6-membered rings. A-cation polyhedra are cubes; six vertices of each cube lie within the layer, and the other two lie directly above and below the A cation. The six anions within the plane of the layering are oxygen atoms of the O1 site; the two anions above and below the A cation are water molecules. From a steric viewpoint, this is an excellent location for the water molecule: a large, open space lies above and below each A-cation polyhedron. From the viewpoint of $R\bar{3}m$ symmetry, the location is somewhat less than ideal: the oxygen atom of each molecule has site symmetry $3m$; the two H atoms of the molecule must therefore be positionally disordered.

The second layer is shown in Figure 2b. In parabariomicrolite, this layer is occupied only by $B1$-cation octahedra. The $B1$–O bonds of these octahedra collectively serve as the sole links between layers of the first type. The second layer has an analogous counterpart in the pyrochlore structure, except that the unoccupied polyhedra of the layer (denoted by the dotted outlines in Fig. 2b) are occupied by A cations in pyrochlore. Thus the pyrochlore structure has extra bonding along Z, absent in parabariomicrolite, which might well account for the lower hardness of parabariomicrolite as compared to microlite. The ϕ-site anions occur at the triple junction of the A-cation polyhedra of this layer. In the pyrochlore structure, with its occupied layer-2 A-cation polyhedra, each ϕ site has bond-valence contributions from one A cation in layer 1 plus three A cations in layer 2, a Pauling bond-strength sum of $4 \times 2/8 = 1$ v.u. The ϕ site of parabariomicrolite receives bond-valence contributions from the A cations of layer 1 only; its Pauling bond-strength sum is only $1 \times 2/8 = 0.25$ v.u. This is the reason why OH and F are typical ϕ-site occupants in pyrochlore, whereas H_2O is the sole ϕ-site occupant in parabariomicrolite.

Several features of the refined structure are noteworthy:

1. Shared polyhedral edges are typically shorter than unshared edges (Table 5).
2. The H_2O molecule is significantly displaced from the ideal position for the ϕ site of the cubic structure of pyrochlore: z(obs.) = 0.315, z(ideal) = 0.375. This conforms with recent refinements of H_2O-bearing pyrochlore (*e.g.*, Groult *et al.* 1982), which show that H_2O in the pyrochlore structure is positionally disordered off the ideal 8*b* position.
3. The presence of A cation *versus* vacancy ordering, which is not compatible with the pyrochlore structure, explains the noncubic symmetry of this mineral. Two criteria for the formation of parabariomicrolite as opposed to bariomicrolite are: (1) an A:B ratio of 1:4, and (2) growth at a low temperature conducive to the incorporation of major amounts of H_2O in the structure. Unlike parabariomicrolite, bariomicrolite should have a A:B ratio in excess of 0.25, crystallizing as either a primary or a secondary pegmatite mineral (*i.e.*, with or without structural water).

On the basis of these two criteria, the Kivu mineral, with a 1:4 A:B ratio and an analysis deficit of 7.7 wt.%, is considered to be parabariomicrolite.

The Status of Type Bariomicrolite

Bariomicrolite was discovered by van der Veen (1963) as a replacement of microlite from a pegmatite near Chi-Chico, Minas Gerais, Brazil. Originally named *rijkeboerite*, it was later renamed *bariomicrolite* by Hogarth (1977) for consistency with the IMA-approved pyrochlore-group nomenclature described therein.

Type bariomicrolite has a somewhat parabariomicrolite-like formula (basis of 4 B cations): $A_{0.78}B_4O_{9.56}(OH)_{2.44} \cdot 2.92H_2O$, where $A = 0.35Ba + 0.14Sn^{2+} + 0.13Fe^{2+} + 0.06U + 0.04Pb + 0.03Ce + 0.01Mn + 0.01Sr$, and $B = 3.38Ta + 0.46Nb + 0.16Ti$. It deviates from parabariomicrolite in its low A-site sum and high H_2O-content, much of which may be due to cation

exchange during heavy-liquid (Clerici solution) separation done prior to the chemical analysis.

The X-ray-diffraction pattern of type bariomicrolite (van der Veen 1963) indicates that it is isostructural with pyrochlore, not parabariomicrolite; however, van der Veen (1963) reported that three additional diffraction-maxima are present in the pattern. These were ascribed to contaminant phases. In light of the parabariomicrolite-like formula and the presence of additional diffraction-maxima in its powder-diffraction pattern, we intend to re-examine type bariomicrolite to determine whether it truly is isostructural with pyrochlore.

Acknowledgements

The authors thank J.S. White of the Smithsonian Institution, Washington and R.I. Gait of the Royal Ontario Museum, Toronto for providing the samples used in this study. Financial support was provided by the Natural Sciences and Engineering Research Council of Canada in the form of a Postgraduate Scholarship to TSE, a University Research Fellowship to FCH, and operating grants to PČ and FCH.

References

Brown, I.D. (1981): The bond-valence method: an empirical approach to chemical structure and bonding. *In* Structure and Bonding in Crystals II (M. O'Keeffe & A. Navrotsky, eds.). Academic Press, New York.

Colby, J.W. (1980): MAGIC V - a computer program for quantitative electron-excited energy dispersive analysis. *In* QUANTEX-Ray Instruction Manual. Kevex Corporation, Foster City, California.

De Almeida, S.C., Johnston, W.D., Jr., Leonardos, O.H. & Pena Scorza, E. (1944): The beryl-tantalite-cassiterite pegmatites of Paraiba and Rio Grande do Norte, northeastern Brazil. *Econ. Geol.* **39**, 206-223.

Eid, A.S. & von Knorring, O. (1976): Geochemical aspects of the tantalum mineral microlite from some African pegmatites. *Res. Inst. Afr. Geol. Univ. Leeds, Ann. Rep.* **20**, 56-58.

Groult, D., Pannetier, J. & Raveau, B. (1982): Neutron diffraction study of the defect pyrochlores $TaWO_{5.5}$, $HTaWO_6$, $H_2Ta_2O_6$, and $HTaWO_6 \cdot H_2O$. *J. Solid State Chem.* **41**, 277-285.

Hogarth, D.D. (1977): Classification and nomenclature of the pyrochlore group. *Amer. Mineral.* **62**, 403-410.

London, D. (1984): Experimental phase equilibria in the system $LiAlSiO_4$-SiO_2-H_2O: a petrogenetic grid for lithium-rich pegmatites. *Amer. Mineral.* **69**, 995-1004.

Pough, F.H. (1945): Simpsonite and the northern Brazilian pegmatite region. *Geol. Soc. Amer. Bull.* **56**, 505-514.

Rucklidge, J.C. & Gasparrini, E. (1969): Specifications of a computer program for processing electron microprobe analytical data (Empadr VII). *Department of Geology, Univ. Toronto, Toronto, Ontario.*

van der Veen, A.H. (1963): A study of pyrochlore. *Nederlands Geol. Mijnbouw, Genootschap Verhand., Geol. Ser.* **22**.

Wiles, D.B. & Young, R.A. (1981): A new computer program for Rietveld analysis of X-ray powder diffraction patterns. *J. Appl. Cryst.* **14**, 149-151.

Yagi, K. & Roth, R.S. (1978): Electron-microscope study of the crystal structures of mixed oxides in the systems Rb_2O-Ta_2O_5, Rb_2O-Nb_2O_5 and K_2O-Ta_2O_5 with composition ratios near 1:3. I. Stacking characteristics of MO_6 layers. *Acta Cryst.* **A34**, 765-773.

Received October 23, 1985, revised manuscript accepted July 4, 1986.